A Gage Block Measurement Process Using Single Wavelength Interferometry

John S. Beers

Institute for Basic Standards
National Bureau of Standards
Washington, D.C. 20234

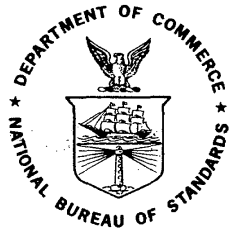

U.S. DEPARTMENT OF COMMERCE, Rogers C. B. Morton, *Secretary*

James A. Baker, III, *Under Secretary*

Dr. Betsy Ancker-Johnson, *Assistant Secretary for Science and Technology*

NATIONAL BUREAU OF STANDARDS, Ernest Ambler, *Acting Director*

Issued December 1975

Library of Congress Cataloging in Publication Data

Beers, John S.
A Gage Block Measurement Process Using Single Wavelength Interferometry.

(National Bureau of Standards Monograph; 152)
Bibliography: p.
Supt. of Docs. No.: C13.44:152
1. Gage Blocks—Calibration. 2. Interferometer. I. Title. II. Series: United States. National Bureau of Standards. Monograph; 152.
QC100.U556 No. 152 [TJ1166] 602'.1s [530'.8] 75-619353

National Bureau of Standards Monograph 152

Nat. Bur. Stand. (U.S.), Monogr. 152, 34 pages (Dec. 1975)
CODEN: NBSMA6

U.S. GOVERNMENT PRINTING OFFICE
WASHINGTON: 1975

For sale by the Superintendent of Documents, U.S. Government Printing Office, Washington, D.C. 20402
(Order by SD Catalog No. C13.44:152). Price 85 cents. (Add 25 percent additional for other than U.S. mailing).

Contents

A Gage Block Measurement Process Using Single Wavelength Interferometry

John S. Beers

The interferometric transfer of the length unit from its defined wavelength to NBS reference standard gage blocks is basic to the gage block calibration program at NBS. The interferometric measurement process using a laser light source and a Kosters type gage block interferometer is described here. Continuous evaluation and refinement of the process is aided by statistical treatment and control chart techniques. All error sources, both random and systematic, are evaluated and the process is maintained in a state of statistical control.

Key words: Calibration; gage blocks; interferometry; laser; length; measurement process; uncertainty.

1. INTRODUCTION

Gage block calibration at NBS depends on the interferometric measurements by which the unit of length is transferred from its defined wavelength of light to the NBS gage block reference standards used for the intercomparison process [1, 2][1].

Although the interferometric process has undergone changes, the new process does not differ fundamentally from previous gage block interferometry at NBS except for using a laser light source. It employs some new techniques and some techniques successfully used in the past coupled with an analysis program designed to reveal random and systematic errors. The analysis program fosters refinements aimed at reducing these errors. A practical limit is eventually reached in making refinements, but the analysis program is continued to assure the reliability of the measurement process.

Briefly, static interferometry is employed to compare NBS gage block reference standards with a laser wavelength. The blocks are wrung to a platen and mounted in an interferometer maintained in a temperature controlled environment. The fringe pattern is photographed and at the same moment those ambient conditions are measured which influence block length and wavelength. A block length computed from these data is a single point in a collection of measurements. By least squares fitting, this collection gives an estimate of process precision, a rate of change of length with time and an accepted value for the correction to the block length at any given time.

1. Figures in brackets indicate the references at the end of this paper.

Gage block length in this measurement process is defined as the perpendicular distance from a gaging point on the top face of the block to the plane surface of identical material and finish wrung to the bottom face. This definition has two advantages. First, specifying a platen identical to the block in material and surface finish minimizes phase shift effects which may occur in interferometry. Second, it duplicates practical usage where blocks of identical material and finish (from the same set) are wrung together to produce a desired length.

The NBS gage block reference standards are commercially produced gage blocks and possess no unusual qualities except that they do have a history of calibration from frequent and systematic comparison with wavelengths of light. Although this description is for blocks from 5 to 20 inches long, a similar process is being applied to blocks less than 5 inches in length.

2. THE INTERFEROMETER

A Kosters type gage block interferometer, shown schematically in figure 1, is used.

The light beam from laser A passes through polarization isolator B and spatial filter B', is diverged by lens C, converged by lens D through aperture E, where it diverges again to fill the field of the interferometer and is collimated by lens F. Entrance aperture E is at the principle focus of lenses D and F. The collimated beam is directed by constant deviation prism G* to beam splitter H where the beam is divided into two beams of equal intensity by the semi-reflecting upper surface. One beam (the measuring beam) continues through to gage block surface K, and optical flat L, and the other beam (reference beam) is reflected through compensating plate I to plane mirror J. Now the beams are reflected by mirror J, gage block surface K, and optical flat L, and are recombined at the beamsplitter. The remaining portions of these beams (some light is lost at each reflection) are visible through lens M and aperture N as an interference pattern created by the phase relationships of the wavefronts in the recombined beams.

Interference in this instrument is most readily explained by assuming that an image of reference mirror J is formed at J' by the beamsplitter. A small angle, controlled by adjustment screws on table P, between the image and the gage block-platen combination creates a Fizeau fringe pattern. When this wedge angle is properly adjusted for reading a gage block length, the interference pattern will appear as in figure 2.

Table P has its center offset from the optical axis and is rotatable by remote control. Several blocks can be wrung to individual small platens or a single large platen and placed on the table to be moved, one at a time, into the interferometer axis for measurement.

---

*This prism separates the spectral lines of quasi-monochromatic light sources such as Hg_{198} for multiple wavelength interferometry.

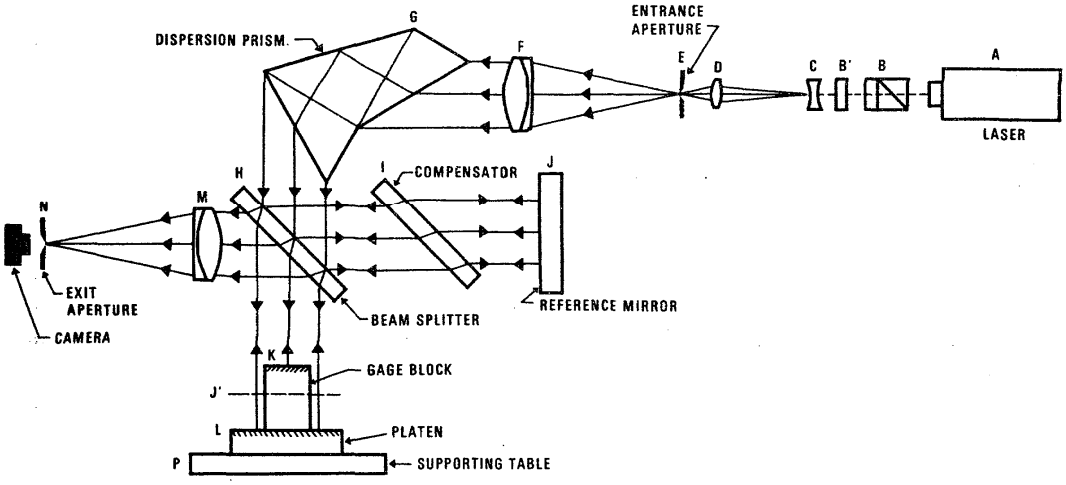

Figure 1. Gage block interferometer.

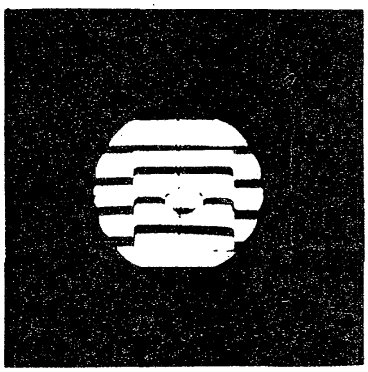

Figure 2. Typical gage block fringe pattern.

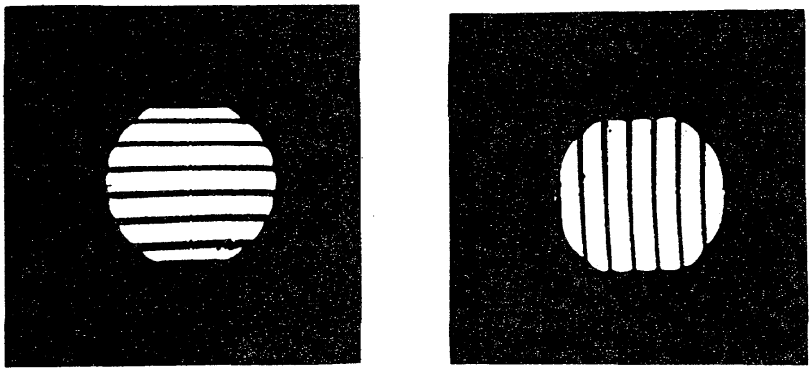

Figure 3. Fringe patterns on a master optical flat.

Two criteria must be met to minimize systematic errors originating in the interferometer: (1) the optical components must be precisely aligned and rigidly mounted and (2) the optical components must be of high quality, i.e. the reference mirror and beam splitter must be plane and the lenses free of aberrations.

Alignment is attained when the entrance aperture, exit aperture and laser beam are on a common axis normal to, and centered on, the reference mirror. This is accomplished with a Gaussian eyepiece, having a vertical and a horizontal crosshair, temporarily mounted in place of the exit aperture, and a vertical and a horizontal crosshair permanently mounted on the reference mirror and intersecting at its center. Through a process of autocollimation with illumination at both entrance aperture and Gaussian eyepiece, the reference mirror is set perpendicular to an axis through the intersections of the two sets of crosshairs and the entrance and exit apertures are set coincident with this axis. In addition, the laser beam is aligned coincident with the axis and the prism adjusted so the laser light coming through the entrance aperture is aligned precisely with the exit aperture. Having an exact 90° angle between the measuring leg and the reference leg is not essential as can be seen from instrument geometry. This angle is governed by the beam splitter mounting. All adjustments are checked regularly to assure their permanence. The gage block and its platen are easily aligned by autocollimation at the time of measurement and no fringes are seen until this is done. Final adjustment is made while observing the fringe pattern, producing the configuration of figure 2.

Overall optical quality is tested by evaluating the fringe pattern produced on a master optical flat mounted on support table P. Photographs showing fringes oriented vertically and horizontally are shown in figure 3. Measurements of the fringe pattern indicate a total distortion of 0.10 fringe vertically in the field. A correction factor proportional to the section of field used can be computed and applied. This correction is relatively small because the field section used in fringe fraction measurement is small. Alternatively, the most likely source of distortion, reference mirror J, can be replaced or reworked, and this course will be taken.

Temperature stability of the interferometer and especially of the gage block being measured is important to precise measurement. For this reason an insulated housing encloses the entire interferometer to reduce the effects of normal cyclic laboratory air temperature changes, radiated heat from associated equipment, operator, and other sources. A box of 3/4 inch plywood with a hinged access door forms a rigid structure which is lined with 1 inch thick foam plastic. Reflective aluminum foil covers the housing both inside and outside.

2.1. Interferometer Corrections

In some interferometers, the entrance and exit apertures are off the optic axis so light falls obliquely on the gage block. Gage block length is then a cosine function of the obliquity angle. In this interferometer

the apertures are precisely on the optic axis, the obliquity angle is zero, and thus no correction is needed. Periodic interferometer alignment insures that the obliquity angle remains zero.

In most interferometers, the entrance aperture is of finite size, therefore ideal collimation does not occur and oblique incidence effects arise from the resultant of all rays from the aperture area. A laser as used with this interferometer is almost a point source because the aperture is at the common focal point of lens D, and collimating lens E, and at this point the beam diameter is the effective aperture.

In two papers, one by Bruce [3] and one by Thornton [4], the authors developed aperture correction equations which consider obliquity of rays from a finite aperture and fringe intensity distribution. Correction factor δ_2, for a gage block of length ℓ, measured with wavelength λ, using a circular aperture is

$$\delta_2 = \frac{\lambda}{4\pi} \tan^{-1} \frac{S(v) - \frac{1}{v}\int_0^v S(v)dv}{C(v) - \frac{1}{v}\int_1^v C(v)dv}$$

where

$$v = \sqrt{\frac{4\ell}{\lambda}} \frac{a}{2f}$$

for aperture of diameter a, and collimating lens of focal length f. S(v) and C(v) are Fresnel integrals. As aperture diameter aproaches zero, the correction approaches zero. In this interferometer the correction is very small because the laser beam diameter is small at the aperture.

3. THE LASER LIGHT SOURCE

The advantage of a laser light source lies in its unequalled coherence. Conventional spectral light sources have such low coherence that gage blocks longer than 10 inches have in the past been measured by stepping up from shorter blocks. Laser fringe patterns in this interferometer compared with patterns from other spectral lamps are of superior contrast and definition throughout the length range.

The disadvantage stems from the somewhat unstable wavelength of Lamb dip stabilized lasers. Variations can approach 1 part in 10^7 both short term and long term. This is not serious for most metrological applications but this study required better stability as will be seen later. Commercial Lamb dip stabilized helium neon lasers of nominal .6328 micrometer wavelength were used for most of the measurements described in this paper and their performance was monitored by periodic calibrations. Lamb dip laser calibration and stability has been described by Mielenz, et al [5].

Toward the end of these gage block measurements the newly developed iodine stabilized laser was used. Its stability exceeds that of Lamb dip lasers by at least two orders of magnitude and even exceeds the stability of Krypton 86, the present international length standard. Schweitzer, et al [6] describe this laser and its calibration in detail.

Single wavelength static interferometry in contrast with multiple wavelength interferometry requires that the gage block length be known to within $\pm 1/4$ wavelength ($\pm 1/2$ fringe) either from its history or from another measurement process. This is no problem for NBS reference blocks.

Laser light must not be allowed to reflect back into its own cavity from interferometer optical components because this will disturb the lasing action and may cause a wavelength shift, wavelength dithering or it may stop the lasing altogether. The reflected light is prevented from re-entering the laser by a polarization isolator consisting of a Glan Thompson prism and a quarter wave plate in the beam as it emerges from the cavity (see B, fig. 1). This assembly is tilted just enough to deflect reflections from its faces to the side of the laser exit aperture.

The isolator linearly polarizes the highly elliptical laser output with the G.T. prism, then circularly polarizes it by phase displacement with the quarter wave plate. Light returning to this assembly from dielectric surfaces in the interferometer is reversed in polarization direction by the 180° phase shift at reflection. Thus, light emerging from the isolator polarized in a clockwise direction returns after reflection polarized counterclockwise. It is then linearly polarized by the quarter wave plate at 90° to the polarization plane of the G.T. prism and is diverted away from the laser cavity by the prism's action.

4. ENVIRONMENTAL CONDITIONS AND THEIR MEASUREMENT

Environmental control of the laboratory holds temperature at $20° \pm .05°C$ and water vapor content below 50% relative humidity. Temperature variations within the interferometer housing are attenuated by a factor of about 10 from those in the room thus insuring stability of both interferometer and blocks.

Temperature, atmospheric pressure, and water vapor content of the ambient air in the interferometer light path must be measured at the time the gage block is measured. From these properties the refractive index of the air is calculated and, in turn, the laser wavelength. Gage block temperature is measured so that the length of the block at 20°C, or any other temperature, can be computed.

4.1. Temperature

The measuring system for air and block temperature consists of copper-constantan thermocouples referenced to a platinum resistance thermometer. Figure 4 is a schematic diagram of the system.

A solid copper cube provides a stable reference temperature measured by a Standard Platinum Resistance Thermometer (SPRT) and a Mueller resistance bridge. A well in the cube holds the thermometer stem, the reference thermocouple junction and a liquid of high heat conductivity but low electrical conductivity. There is also a second well whose function will be described later. An enclosed thermocouple selector switch connects the measuring junctions, one at a time, to the reference junction and the

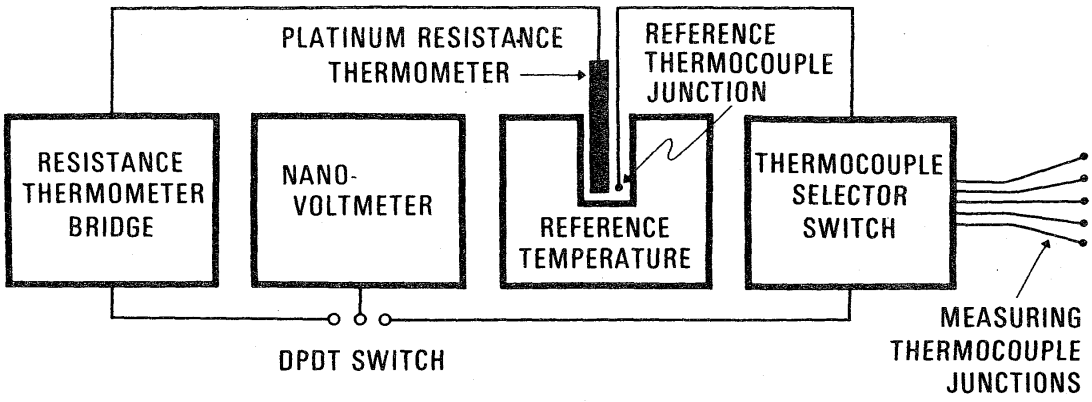

Figure 4. Temperature measuring system schematic.

thermal emfs generated by the temperature differences between measuring junction and reference junction are indicated on a nanovoltmeter. The nanovoltmeter is shared with the bridge where it is used as a nullmeter. To keep the copper block in a stable state and to minimize thermal emfs in the selector switch, both block and switch are enclosed in an insulated box. The switch is operated through a fiber shaft extending to the exterior and the protruding part of the thermometer is protected by an insulated tube.

Thermocouples generate emfs proportional to the temperature gradient along the wire:

$$E = \int_{T_1}^{T_2} \phi dT$$

where T_1 and T_2 are the temperatures of the reference and measuring junctions respectively

ϕ is the thermocouple constant.

Minimizing this gradient reduces uncertainties.

Relating the system to the International Practical Temperature Scale of 1968 (IPTS '68) is a three step procedure. First, the SPRT is calibrated using methods described in NBS Monograph 126 [7]. Second, the bridge is calibrated as described in the same Monograph. The third step is the calibration of the thermocouples which is accomplished with a second SPRT and insulated copper cube. The second cube has an extra well for thermocouples being calibrated and is heated one or two degrees to equilibrium. Measured thermal emfs generated by the temperature difference between the two cubes together with the temperatures of the cubes allow computation of a calibration factor for each junction.

Integrity is maintained by periodic redeterminations of the SPRT ice point with a triple point cell, checking the bridge against a calibrated standard resistor and checking the thermocouples for equality when they are all at the same temperature in a well of an insulated copper cube.

4.2. Atmospheric Pressure

The interferometer housing is not airtight and pressure inside it is the same as laboratory pressure. An aneroid barometer is located adjacent to and on the same elevation as the interferometer. Aneroid barometers can be read much faster than mercury barometers and this is an important characteristic in interferometric length measurements. The aneroid used for gage block measurements has good stability, and frequent comparisons with NBS reference barometers insure its relial

4.3. Water Vapor

A commercially available Dunmore type hygrometer is used. This type has a sensing element whose electrical resistance changes with moisture content of the air. Periodically calibrated, it has an uncertainty of about 1.5% relative humidity [8, 9]. The sensing element was originally mounted adjacent to the interferometer, but was later moved inside the interferometer housing (see section on process evaluation).

5. GAGE BLOCK MEASUREMENT PROCEDURE

In preparation for measurement, the gaging faces of the NBS standards are cleaned with trichloroethylene and ethyl alcohol. Wiping the alcohol-rinsed gaging faces is done with paper tissue or a clean cotton towel. Lint or dust is removed with a camel's hair brush.

The gaging faces are examined for burrs and, if present, these are removed with a deburring stone. The bottom end is tested for wringability with a quartz optical flat. The transparency of the flat makes possible a judgment of the wring. A uniform grey color at the interface indicates a good wring. Any colored or light areas indicate a gap of several microinches between the faces in that area, and such a gap may result in an erroneous length measurement. Deburring and cleaning is continued until a good wring is achieved. The quartz flat is left wrung to the gaging face to keep it clean until preparations are completed for wringing the block to the steel optical flat (platen).

Preparation of the steel platen is similar. Trichloroethylene and ethyl alcohol rinses are used, then deburring if necessary, followed by more rinsing and drying. After sweeping with a camel's hair brush, a thin uniform film of light grease is applied to the wringing surface with a bit of tissue. This film is rubbed and finally polished with tissue or towel until the film appears to be gone. After carefully sweeping the platen with the brush, it is ready for wringing.

The block is removed from the quartz flat and the exposed gaging face

is immediately wrung by carefully sliding it onto the edge of the steel platen, maintaining perpendicularity by feel. Sliding is continued until wringing resistance is felt, and then with slight downward pressure the block is slowly worked into its final position. Square style blocks, such as the NBS reference standards, are positioned so that the gage point* is at the right in the viewing field of the interferometer. One to four blocks can be wrung to the platen for measurement.

The platen with its wrung blocks is placed in the interferometer and two thermocouples are fed down the center hole of each block, one about three quarters down and one about one quarter down the length of the block. A small wad of polyurethane is pushed into the hole to seal and hold the wires.

A preliminary alignment by autocollimation with the Gaussian eyepiece as the support table is adjusted, will produce fringes. Rapid changes in the fringe pattern occur as the block cools from handling.

It is convenient to wring the blocks in late afternoon and allow overnight temperature stabilization. No effort has been made to determine minimum stabilization time. Two length observations are made several hours apart, but the first measurement is not taken until the laser is in equilibrium. Leaving the laser on continuously when observations are being made over several days eliminates delays. The laser beam is blocked from entering the interferometer except when measuring.

Final fringe pattern adjustment is made so that the platen fringes are parallel to the top and bottom edges of the block and one fringe on the block goes through its defined gage point. The direction of increasing fringe order is verified by pressing down on the eyepiece and observing fringe flow. A photograph is taken of the pattern. Block temperature, air temperature, barometric pressure, and humidity are measured immediately before and after the photograph and then averaged.

The photograph can be either a positive or a negative and image size is determined by the distance between the film plane of the lensless camera and the viewing aperture of the interferometer. A compromise is made between image size and exposure time, but short exposure is desirable because the fringe pattern may shift. Further image magnification takes place in the fringe measuring instrument. A compromise is also made between magnification in the photograph and magnification in the measuring instrument. Too much total magnification degrades image sharpness.

---

*NBS rererence standards in the 5 to 20 inch size range are of the square type with an axial hole, and the gage point is on the measuring face midway between the edge of the hole and the edge of the block nearest the size marking. In figure 2 the right hand edge is the reference edge and the gage point is midway between it and the right hand edge of the hole. In sizes below 5 inches the reference standards are of the rectangular type with the gage point at the center of the measuring face as in figure 5.

Fringe fractions are taken from the photograph with a coordinate comparator which has a fixed stage in the focal plane of a microscope movable on X-Y slides by precision screws having drum readouts. Four measurements of distances "a" and "b" are recorded and averaged to obtain fringe fraction f, figure 5. Settings on the block fringe to obtain "a" are made at the point where the fringe intersects the gage point. Settings on the platen fringes to obtain "a" and "b" are made as close as practical to the edges of the block because it is here that the platen best represents an extension of the bottom face of the block. Parallelism between gage block and platen is also read from the photo because this information is useful in detecting a defective wring. Poor wringing contact is indicated if the parallelism is different from its usual value and this is sufficient cause to discard a particular length measurement.

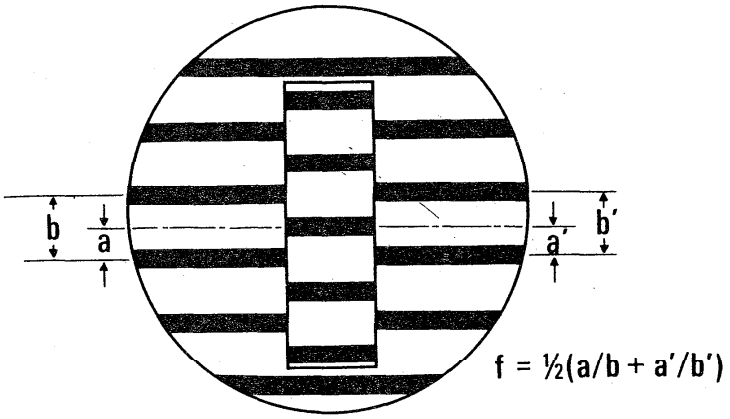

Figure 5. Fringe fraction measurement.

Photographing fringe patterns has several advantages. The photograph is a permanent record which can be reinterpreted at any time with the same or other techniques. Changes in block geometry are readily seen by comparing photographs in time sequence. The coordinate comparator is superior to the common practice of fringe fraction estimation by eye because it is more objective, lends itself to multiple measurements and averaging, and is more precise. Finally, photography is fast and thus permits readings of the ambient conditions to closely bracket the fringe recording. This is especially important because atmospheric pressure is usually in a state of flux.

6. COMPUTATION OF GAGE BLOCK LENGTH

Calculating gage block length from the data is done in 3 steps:

(1) Calculation of wavelength, λ_{tpf}, at observed ambient conditions.

(2) Calculation of the whole number of fringes in the gage block length from its predicted length and the laser wavelength in ambient air.

(3) Calculation of the gage block length from the whole number of fringes, the observed fringe fraction, wavelength in ambient air, gage block temperature, and interferometric correction factors.

6.1. Calculation of Wavelength

Edlen's 1966 formula [10] for the refractive index of air is used to calculate the wavelength from the relationship

$$\lambda_0 = n_{tpf}\lambda_{tpf}$$

as follows

$$\lambda_{t,p,f} = \frac{\lambda_0}{n_{t,p,f}} = \lambda_0\ [1+A\cdot B-C]^{-1}$$

where

$$A = \frac{P[8342.13 + 2406030\ (130-\sigma^2)^{-1} + 15997\ (38.9-\sigma^2)^{-1}]\ 10^{-8}}{720.775}$$

$$B = \frac{1 + P\ (0.817-0.0133t)\ 10^{-6}}{1 + 0.003661t}$$

$$C = f\ (5.7224-0.0457\sigma^2)\ 10^{-8}$$

Symbols:

λ_0 = Vacuum wavelength in μm

$\lambda_{t,p,f}$ = Wavelength at observed conditions t,p,f

$n_{t,p,f}$ = Index of refraction of air at t,p,f

p = Atmospheric pressure in mm of Hg

t = Temperature in degrees Celsius

f = Water vapor pressure in mm of Hg

$\sigma = 1/\lambda_0$ in μm^{-1}

6.2. Calculation of the Whole Number of Fringes

This method for determining the whole number of fringes is valid only if the block length is known to better than $\pm 1/2$ fringe (1 fringe $\approx$ 12μin. for helium neon laser light) from either its history or from an independent measurement process. The calculation is as follows:

$$F = \frac{2\, L_p [1+C(t'-20°)]}{\lambda_{tpf}}$$

where F is the number of interference fringes in the length of the block at temperature t', and in air of temperature t, pressure p, and vapor pressure f.

L_p is the predicted block length at 20°C taken from an independent measurement or from the block's history.

C is the linear thermal expansion coefficient per degree Celsius of the block.

t' is the block temperature at the time of measurement.

λ_{tpf} is the wavelength in the ambient air at the time of measurement.

The fractional part of F is retained temporarily for the reason explained below.

6.3. Calculation of Block Length from the Observed Data

Generally, the observed fringe fraction ϕ is simply substituted for the fractional part of F, but there are cases where the last digit in whole number F must be raised or lowered by one. For example if the retained fractional part of F is .98 and the observed fraction is .03, obviously the last whole number in F must be raised by one before substituting the observed fraction.

The new measured block value, in fringes, is

$$F' = F + \phi$$

Finally, the interferometer aperture correction, δ_2, is added, the block is normalized to 20°C, and a conversion to length units is made to arrive at the final value at 20°C as follows:

$$L_{20°} = \frac{\lambda_{tpf}}{2}\, F'[1+C(20°-t')] + \delta_2$$

7. SYSTEMATIC AND RANDOM ERRORS

Potential sources of systematic errors are as follows·

(1) Wavelength

a. Vacuum wavelength of laser

b. Refractive index of air equation

c. Refractive index determination

1. Air temperature measurement

2. Atmospheric pressure measurement

3. Humidity measurement

(2) Interferometer

a. Alignment

b. Aperture correction

c. Obliquity angle correction

(3) Gage Block

a. Gage block temperature measurement

b. Thermal expansion coefficient

c. Phase shift difference between block and its platen.

Length proportional errors are potentially the most serious in long block measurement. Their relative influence is illustrated in table 1. One example will help explain the table: if air temperature measurement is in error by 0.1°C a systematic error of 1 microinch (1 part in 10^7) results in the value of a 10 inch gage block.

Every practical means, as previously discussed, was used to reduce these errors to a minimum and, at worst, errors in measuring the parameters listed in the table did not exceed those listed in column 1 (1 μin. or 1 part in 10^7), and most are undoubtedly in the column 2 category. Further evaluation of these errors is described in the section on process evaluation.

A few error sources in the first list but not in the table have not been completely discussed. The first of these is phase shift difference between block and platen. As indicated earlier, the present solution is to closely match the optical characteristics of block and platen. This undoubtedly reduces the phase shift difference to a point where it becomes

TABLE 1. LENGTH DEPENDENT ERRORS RESULTING FROM SYSTEMATIC ERRORS IN MEASUREMENT PARAMETERS

PARAMETER	ERROR IN A 10 INCH GAGE BLOCK 1 microinch (1 part in 10^7)	0.1 microinch (1 part in 10^8)
Wavelength		
Vacuum wavelength	1 part in 10^7	1 part in 10^8
Refractive index formula	1 part in 10^7	1 part in 10^8
Air temperature	0.1°C	0.01°C
Atmospheric pressure	0.30 mm	0.03 mm
Relative humidity	12% R.H.	1.2% R.H.
Interferometer		
Alignment	0.45 mm/m	0.14 mm/m
Gage block		
Steel gage block temperature	0.01°C	0.001°C

smaller than measurement process precision and, therefore, difficult to detect. Future studies will deal with the problem of phase shift, especially those cases where block and platen properties cannot be matched.

Thermal expansion coefficients of gage blocks have an uncertainty that is to a large extent nullified by measuring at temperatures very close to the 20°C reporting temperature. Gage block manufacturers give 11.5×10^{-6}/°C for steel blocks. This average value may be uncertain by 5% ($.6 \times 10^{-6}$/°C) for individual blocks. The manufacturer's value was used for the 10 inch steel control block described in the next section and for all NBS steel reference standards. A program is now in progress to measure coefficients at NBS.

Random errors arise from variability in any parameter in table 1, and in addition, they can arise in the fringe fraction measurement and wringing variability.

8. PROCESS EVALUATION

A collection of values from repetitive measurements of stable control standards can be characterized by (1) the limiting mean value, (2) process precision, (3) systematic error and (4) process uncertainty. Furthermore, these values can be plotted against a time base to produce a control chart showing the limiting mean and process precision. The basic assumption in most statistical techniques is that the data are a random sample from a stable probability distribution, and in most cases that they have a normal (Gaussian) frequency distribution. This assumption can be tested by the

control chart method and if it meets the test, the process is said to be in a state of statistical control.

These are powerful tools for process evaluation because the effects of planned process changes are visible on the control chart and are quantified by the statistics. If measurements of the control standards made after each process change are analyzed as a subgroup the effect, if any, on process precision and limiting mean will be revealed. These methods were used for tracking down error sources, evaluating precision, and indicating the way to improved measurement techniques.

8.1. Control Standards

Four gage blocks were selected as control standards to evaluate and improve this interferometric measurement process. The blocks and their purposes are as follows:

(1) A 0.150 inch chrome-carbide gage block. This block is short enough to minimize the influence of variations and uncertainties in wavelength, temperature, pressure and humidity. Repeated measurements tend to show the best precision attainable with this process.

(2) A 0.129 inch steel gage block selected for the same reasons as above, but in addition because it had slightly superior geometric and surface finish characteristics. It is an alternate control block and was not available at the beginning of the experiment.

(3) A 10 inch glass-ceramic gage block stack consisting of two 3 inch and one 4 inch block wrung together (a single 10 inch block of this material was not available). This block has a very low thermal expansion coefficient thus minimizing the influence of block temperature uncertainties but accentuating, by virtue of its relatively long length, uncertainties in wavelength, air temperature, pressure, and humidity.

(4) A 10 inch steel gage block. This block is equally affected by all the parameters that contribute to the uncertainties of the 10 inch glass-ceramic block, and in addition, by the uncertainties of temperature and thermal expansivity.

Each of the four blocks was wrung to its own steel optical flat and remained wrung throughout the evaluation so that wringing variability would not obscure the investigation of other parameters. The 0.129 inch block was wrung to a steel flat of matching surface finish. A 0.150 inch steel block was wrung to the upper gaging face of the glass-ceramic block to make fringe contrast and definition comparable to the other control blocks. Thermal expansion of this steel auxiliary block was included in computations of the length.

8.2. Determining Process Characteristics

The first step was to determine process characteristics existing during prior measurements of the NBS long block reference standards by

single wavelength interferometry. Data for the first control standard measurement subgroup was therefore obtained before making any planned process changes.

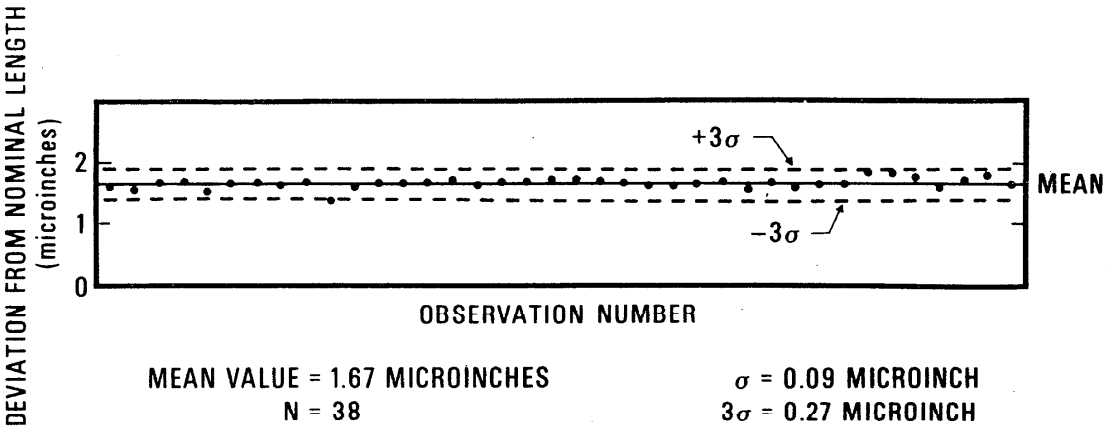

Figure 6. Control chart on the 0.129 inch control standard.

Figure 6, a typical control chart, is for the 0.129 inch block and it shows individual measurement values expressed as deviations from nominal length (corrections) at 20°C plotted against observation number. The solid line is the mean value for the set and the dashed boundary lines are located ± 3 standard deviations ($\pm 3\sigma$) about the mean. The two 10 inch blocks have many more points taken over a long time period so, for convenience, figure 7 shows only averages of subgroups with their $\pm 3\sigma$ bandwidths and plotted against a time scale. Figure 8 is a similar chart for the 0.150 and 0.129 inch blocks. Table 2 summarizes process characteristics and lists process changes for each subgroup.

8.3. The Search for Systematic Errors

Time period A on the chart (fig. 7) and in table 2 shows representative process characteristics for the "as it was" evaluation. Once these were established, the next steps were devoted to searching for systematic errors.

First, an analysis was made on data from period A. Coefficients of linear dependence were computed for control block values against air temperature, barometric pressure, relative humidity, and gage block temperature. The analysis revealed significant dependence (see fig. 9) between the 10 inch control block values and relative humidity. Humidity corrections were apparently incorrect. Two causes were possible: an error in the vapor pressure term in the refractive index equation or an error in humidity measurement. After verifying that the correct equation was used, a measurement error was investigated by using two hygrometers; one inside and one outside the interferometer housing. It was discovered that

TABLE 2. SUMMARY OF CONTROL STANDARD MEASUREMENTS

10 INCH STEEL CONTROL STANDARD

TIME PERIOD Letter Designation	MONTH	N	MEAN VALUE (μin.)	σ^2 $(\mu in.)^2$	σ (μin.)	3σ (μin.)	PROCESS CHANGE
A	0	20	20.0	0.384	0.62	1.86	
B	1	20	19.8	0.116	0.34	1.02	Humidity measurement changed
C							
D ← omitted	6	20	19.9	0.102	0.32	0.96	Temperature system rebuilt
E							
F	8	25	19.7	0.032	0.18	0.54	Heat source moved
G	11	4	19.4				Laser No. 109 failed
H	13	10	19.0	0.041	0.20	0.60	Laser No. 184 used
I	14	10	18.7	0.051	0.23	0.69	No change
J	23	10	18.4	0.052	0.23	0.69	No change
K	24	24	18.6	0.045	0.21	0.63	Iodine stabilized laser used
L	25	10	17.9	0.014	0.12	0.36	Laser No. 184 used
M	25	10	18.7	0.045	0.21	0.63	Iodine stabilized laser used
N	26	10	18.2	0.040	0.20	0.60	Laser No. 184 used
O	26	10	18.7	0.033	0.18	0.54	Iodine stabilized laser used
P	29	20	18.8	0.036	0.19	0.57	No change
Q	31	12	18.6	0.022	0.15	0.45	Laser 184-new calibration
R	32	10	18.9	0.022	0.15	0.45	Iodine stabilized laser used
K thru R	24-32	74	18.7	0.048	0.22	0.66	Summary of all iodine stabilized laser values
J thru Q	23-31	42	18.3	0.098	0.31	0.93	Summary of all corresponding laser No. 184 values

Continued

Table 2 Continued

10 INCH GLASS-CERAMIC CONTROL STANDARD

TIME PERIOD Letter Designation	MONTH	N	MEAN VALUE (μin.)	σ^2 $(\mu in.)^2$	σ (μin.)	3σ (μin.)	PROCESS CHANGE
A	0	25	26.2	0.518	0.72	2.16	
B	1	20	25.9	0.026	0.16	0.48	Humidity measurement change
C							
D ←omitted	6	18	25.9	0.058	0.24	0.72	Temperature system rebuilt
E							
F	8	26	26.0	0.044	0.21	0.63	Heat source moved
G	11	4	26.1				Laser No. 109 failed
H	13	10	25.8	0.057	0.24	0.72	Laser No. 184 used
I	14	10	25.5	0.037	0.19	0.57	No change
J	23	10	26.3	0.063	0.25	0.75	No change
K	24	24	27.2	0.030	0.17	0.51	Iodine stabilized laser used
L	25	10	26.6	0.035	0.19	0.57	Laser No. 184 used
M	25	10	27.3	0.020	0.14	0.42	Iodine stabilized laser used
N	26	10	26.9	0.025	0.16	0.48	Laser No. 184 used
O	26	10	27.4	0.036	0.19	0.57	Iodine stabilized laser used
P	29	20	27.5	0.031	0.18	0.54	No change
Q	31	12	27.1	0.047	0.22	0.66	Laser 184-new calibration
R	32	10	27.4	0.029	0.17	0.51	Iodine stabilized laser used
K thru R	24-33	74	27.4	0.040	0.20	0.60	Summary of all iodine stabilized laser values
J thru Q	23-31	42	26.7	0.134	0.37	1.11	Summary of all corresponding laser No. 184 values

Continued

TABLE 2 (continued)

0.150 INCH CONTROL STANDARD

TIME PERIOD Letter Designation	MONTH	N	MEAN VALUE (μin.)	σ^2 $(\mu in.)^2$	σ (μin.)	3σ (μin.)
A thru B	0- 3	48	0.74	0.011	0.10	0.31
C thru F	6- 8	28	0.64	0.024	0.15	0.46
K thru M	24-25	38	0.37	0.009	0.09	0.28

0.129 INCH CONTROL STANDARD

TIME PERIOD Letter Designation	MONTH	N	MEAN VALUE (μin.)	σ^2 $(\mu in.)^2$	σ (μin.)	3σ (μin.)
F	8	28	2.06	0.009	0.10	0.30
K thru M	24-25	38	1.67	0.008	0.09	0.27

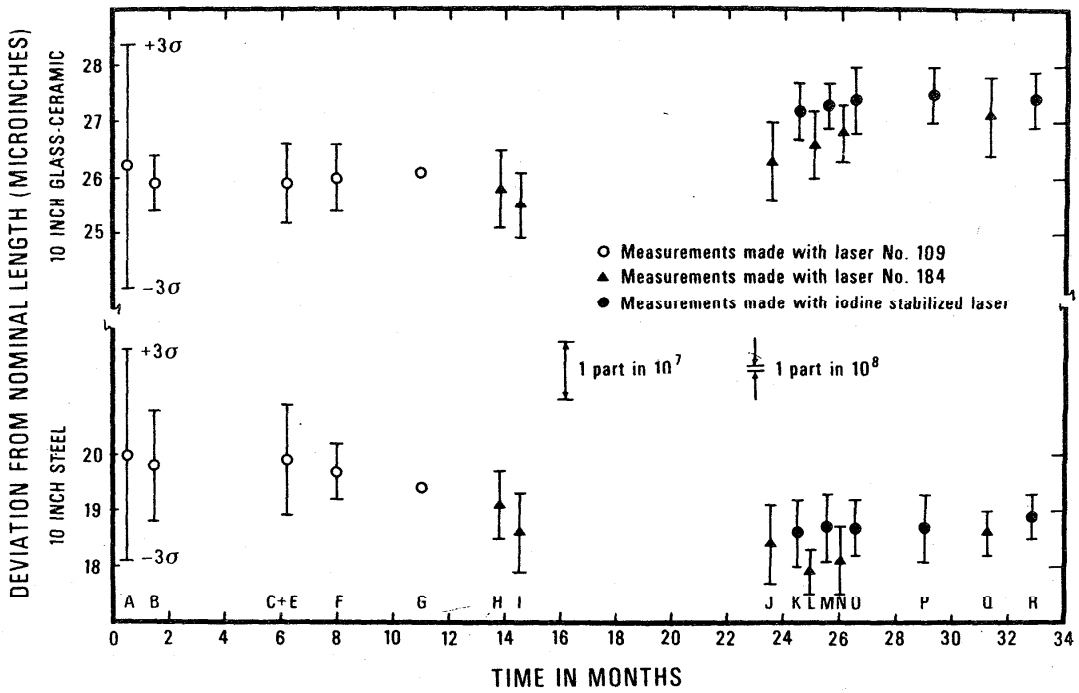

Figure 7. Control charts on the 10 inch steel and 10 inch glass-ceramic control standards.

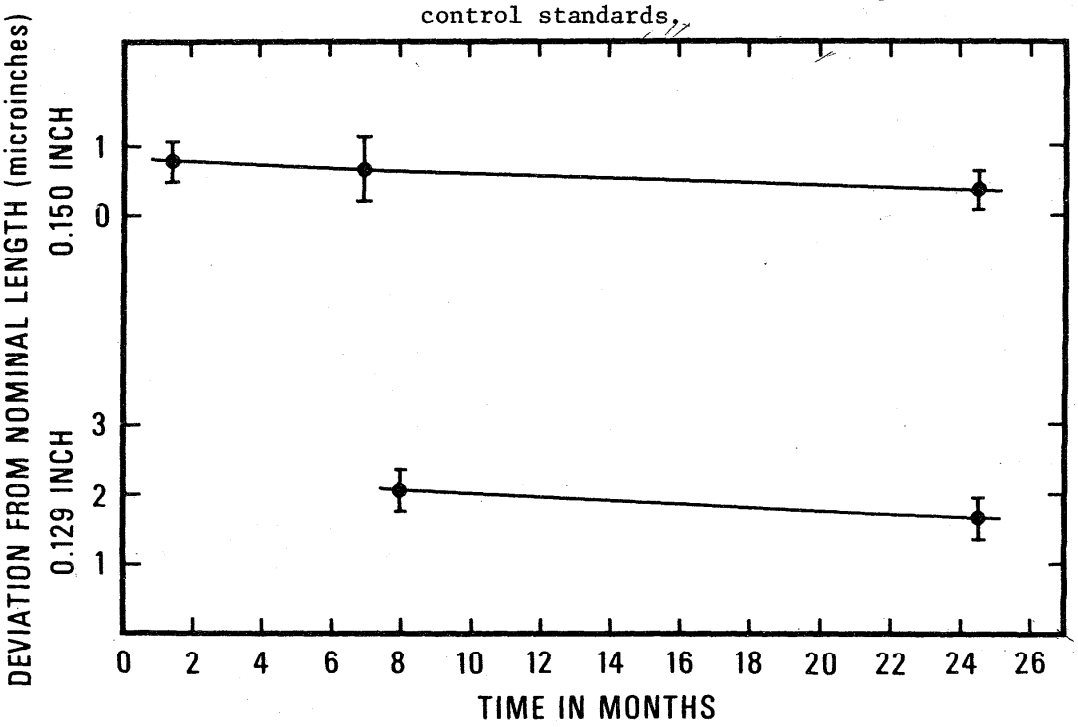

Figure 8. Control charts on the 0.129 and 0.150 inch control standards showing secular changes.

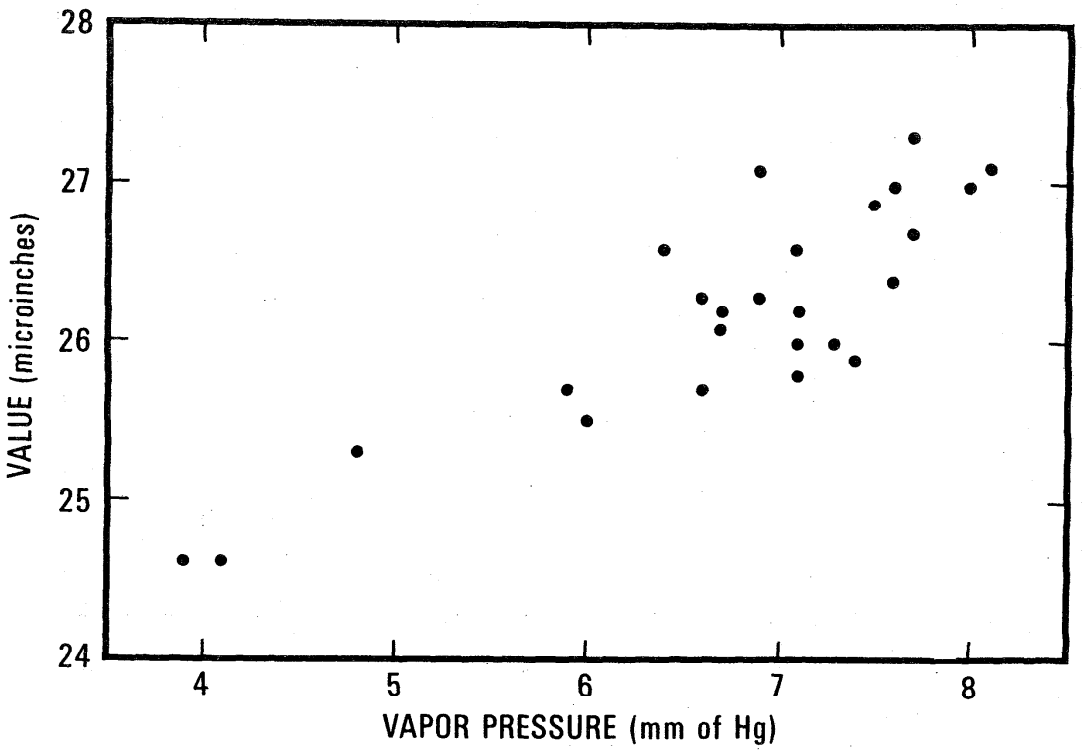

Figure 9. Correlation chart, length vs vapor pressure.

although both instruments gave the same reading with the interferometer door open, a difference developed once the door was closed. Hygroscopic material in the housing is the probable explanation.

The hygrometer sensing element was then mounted inside the housing (a process change) and control block measurements were resumed for period B. A marked improvement in precision was obvious on the control charts (fig. 7) but no significant change in mean values occurred.

Period B measurements, no longer masked by imprecise humidity measurements, indicated the steel block values to be less precise than the glass ceramic values. Temperature was the only parameter likely to affect steel more than glass-ceramic, therefore, it was possible that temperature measurement variability was causing the difference in precision. This theory was tested by attempting to improve the temperature measuring system. New thermocouples were assembled using higher grade copper and constantan wire and the lead length was reduced by moving the reference temperature enclosure from a position several feet away to a position in contact with the interferometer housing. The leads do not pass through open air, but go directly into the housing with a consequent improvement in thermal environment for the thermocouple system. Finally, one measuring junction was attached to the stem adjacent to the resistance coil of the SPRT. This allows verification of temperature equality between reference

junction and thermometer coil and checks for the presence of parasitic thermal emfs. The new temperature system was then recalibrated by the method previously described.

Control standard measurements were resumed and results plotted on the control charts, periods C and E. Points taken in period D were omitted from this subgroup for cause.* It seemed apparent from the control chart that no improvement in precision resulted from rebuilding the temperature system, in fact precision was degraded slightly.

In rebuilding the temperature system, the nanovoltmeter was moved close to the interferometer from a location several feet away. Even though circuitry is solid state, the small amount of heat generated by this instrument could introduce perturbations effecting precision. Evidence such as a faster rise in interferometer air temperature when power was supplied to the nanovoltmeter plus the metrological axiom against heat sources being near measurement areas led to moving the meter.

Again the effect of this change was visible on the control chart, period F, with a statistically significant improvement in precision for the 10 inch steel control standard, the one most influenced by temperature. Temperature system rebuilding had indeed improved precision. A small systematic error probably not exceeding 0.001°C may be indicated by the change in mean value of the 10 inch steel block but the evidence for this conclusion is marginal.**

Measurement precision on the 10 inch blocks (σ=0.18 and 0.21 μin.) now approached that of the 0.150 inch control block (σ=0.10 μin.) suggesting that length dependent random errors were very small. Until factors causing this variability are discovered it is unlikely that process precision can be improved.

Another round, G, was started with no process changes. Only four measurements were made before laser No. 109 broke down, requiring a new plasma tube. Unfortunately this occurred just before a planned laser calibration which would have allowed evaluation of wavelength, the last source of systematic error remaining to be studied. Judgment of long term stability of this laser must be based mainly on three calibrations: one at the beginning of this study and two about 18 months before. Vacuum wavelength variations of approximately 1 part in 10^8 were observed. Extrapolation of this evidence is not advisable although the control block data seems to reinforce the picture of a well behaved laser.

At this point measurement precision (3σ) of the process was about 5

*During this period, the aneroid barometer was carried back and forth between two laboratory rooms. A periodic barometer check indicated a calibration change, probably from mechanical shock. Pinpointing the exact date of the calibration shift was impossible so all values were omitted.

**Further tests of temperature measurement effectiveness are given in the Appendix, item 4.

parts in 10^8 for the 10 inch control blocks. Variations in vacuum wavelength of a few parts in 10^8 became significant at this level. Laser No. 184, newly calibrated, was installed shortly after the demise of No. 109 and periods H, I, J, L, N, and Q (plotted with symbol "▲" in figure 7) were measurements made with No. 184. The somewhat erratic nature of these measurements led to expending much time and effort on an error search that revealed nothing until an iodine stabilized laser became available.

The iodine stabilized laser was used in periods K, M, O, P, and R (plotted with symbol "●" in figure 7). This helium-neon laser slaved to a saturated absorption line of iodine is far more stable than any light source in the visible range now in use including krypton 86, the international standard. The measured vacuum wavelength of the iodine stabilized laser must carry with it the uncertainty in krypton 86, but since this uncertainty is only a few parts in 10^9 it is of no consequence in these gage block measurements.

The differences between the two lasers shows up well in figure 7. Period Q measurements with No. 184 were made immediately after the laser was recalibrated and shows a significant reduction in the systematic difference. Recalibration indicated a change of 13 parts in 10^8 in vacuum wavelength over an 18 month period. This laser was apparently atypical and the measurements made with it were of little value for this study.

The remarkable stability of the iodine stabilized laser is apparent from the data in table 2 and the control charts of figures 7, 10, and 11. Selecting all iodine stabilized laser values from periods K through R, the process precision is 0.66 microinch for the 10 inch steel block, whereas for the comparable periods J through Q it is 0.93 microinch for laser No. 184. Comparable figures for the 10 inch glass ceramic block are 0.60 microinch and 1.11 microinch.

In figures 10 and 11 all iodine stabilized laser values are plotted vs observation number. The analysis of this data for linear dependence against air temperature, barometric pressure, relative humidity, and gage block temperature failed to show significant correlations.

Stability of the two 10 inch control standards is of interest and it can be stated with reasonable certainty that they changed less than 2 microinches (2 parts in 10^7) in the 33 months covered in this report. But the nature of systematic errors discovered during this process study makes it impossible to express the change more precisely or to define the trend of the change. A length change, of course, was not unexpected.

It is significant that all subsequent measurements fell within the approximate ± 2 microinch 3σ bandwidth of group A in spite of the random and systematic errors discovered and remedied in the process analysis.

The 0.150 and 0.129 inch control standards also exhibited time dependent length changes as shown in figure 8. Rates of -0.19 μin./year and -0.28 μin./year for the 0.150 and 0.129 inch block respectively were

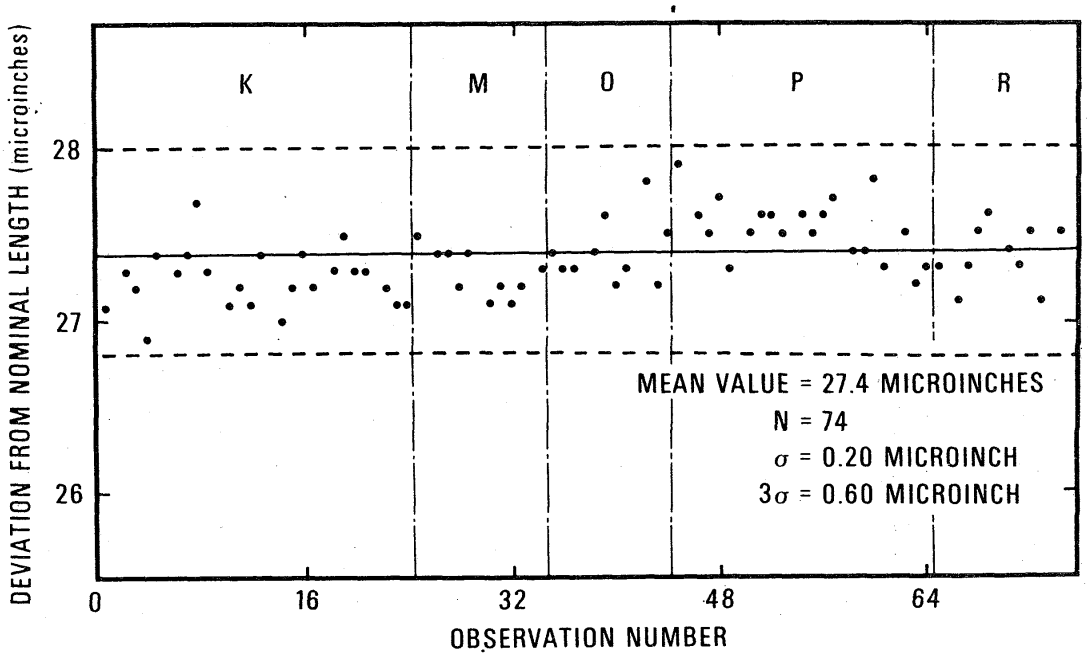

Figure 10. Control chart on the 10 inch glass-ceramic block measured with an iodine stabilized laser.

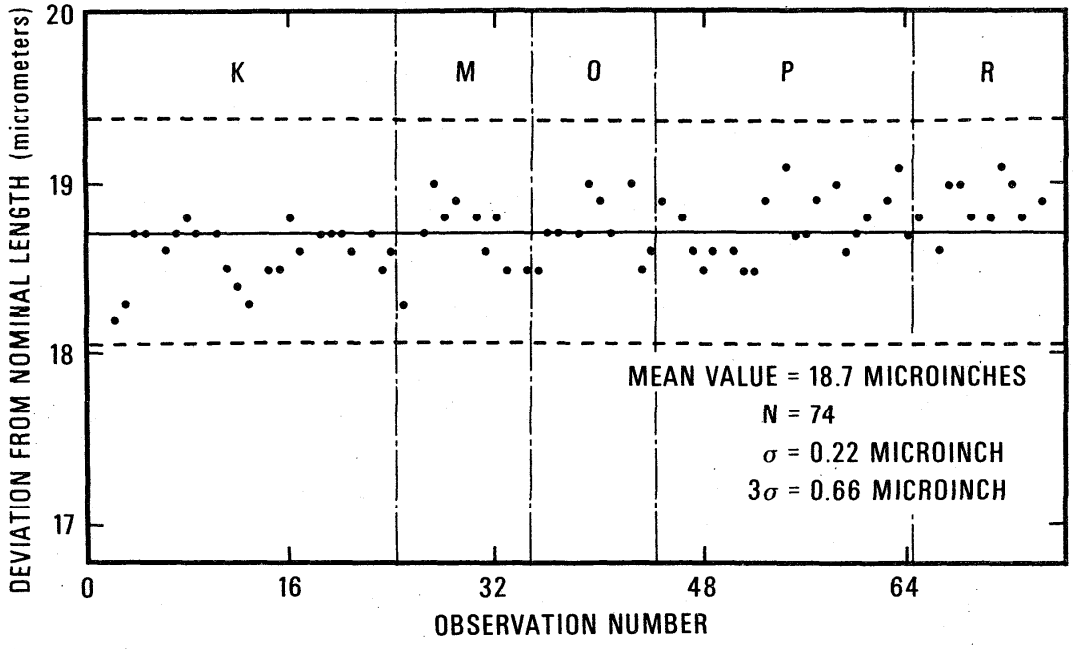

Figure 11. Control chart on the 10 inch steel block measured with an iodine stabilized laser.

determined.

During the search for systematic errors the parametric measuring devices and sources were calibrated and checked. Some were mentioned in this section, others not, but all are summarized in the Appendix.

8.4. The Study of Random Errors

The 0.150 and 0.129 inch blocks were selected as controls because their short lengths reduced length dependent random and systematic errors to insignificance. Thus, the control charts on these blocks demonstrate a nearly minimum random variability that must originate in the only non-length dependent variable, fringe fraction measurement. Knowledge of the minimum variability can be useful in long block error analysis.

Twenty-eight measurements of the 0.129 inch block were studied for clues to minimum random variability. Each photograph was remeasured and the lengths recomputed to create a second set, called Round 2, based on the remeasured fringe fraction. The precisions of the four submeasurements made on each photograph were also computed and pooled. The results are in table 3.

TABLE 3. ANALYSIS OF 28 MEASUREMENTS OF THE 0.129 INCH CONTROL BLOCK

	Round 1	Round 2
Mean deviation from nominal length	2.06 μin.	2.06 μin.
Standard deviation, S_t, of a length value from a single photograph	.097	.096
Variance, S_t^2	.00941	.00922
Standard deviation, S_m, of the difference between Round 1 and Round 2	.067	
Variance, S_m^2	.00449	
Pooled standard deviation, S_s, of the mean of 4 fringe fraction submeasurements of a photograph	.013	
Variance, S_s^2	.00017	

Mean length values for Rounds 1 and 2 agree exactly (2.06 μin.) and the total random errors (S_t=.097 μin. and .096 μin.) agree closely. Two principal components contribute to total random error: fringe fraction measurement error, S_m, coming from the process, and photographic image error, S_p, coming from sources described below. The magnitude of the fringe fraction measurement process error is the standard deviation of the differences between Rounds 1 and 2 (S_m=.067 μin.) and since this is

not as large as S_t there must be a contribution from image variations from photograph to photograph which are not related to the control block length. S_p is computed as follows:

$$S_p^2 = S_t^2 - S_m^2 = (.097)^2 - (.067)^2 = .00492, \; S_p = .070 \; \mu in.$$

Comparing variances S_m^2 and S_p^2 with S_t^2 shows that approximately one-half the total random error comes from the fringe measuring process and the other half from photographic image variations. Image variations from one photograph to the next probably result from several factors such as vibration, surface roughness effects and incomplete spatial filtering of the laser light.

There is a relatively small random error (S_s = .013μin.) in the four submeasurements on a photograph. Thus, the observer tends to interpret the fringes consistently at a given time, but image ambiguities cause the observer to interpret the fringes in a slightly different manner at a later time as indicated by the magnitude of S_p (.070 μin.).

Analyses of variance can also shed light on length dependent random errors. Only data taken with the iodine stabilized laser, where wavelength uncertainties drop out, are used in the following analysis.

Combined pressure and humidity measurement variabilities are determined by comparing the variances of the 0.129 and 0.150 inch blocks with the variance of the 10 inch glass-ceramic block with its maximization of pressure and humidity effects and minimization of temperature effects. Variance, S_{pf}^2, caused by pressure and humidity is

$$S_{pf}^2 = S_{max}^2 - S_{min}^2$$

where S_{max}^2 and S_{min}^2 are variances of the 10 inch glass-ceramic and the 0.150 inch blocks respectively. Then

$$S_{pf}^2 = 0.040 - 0.009 = 0.031 \; \mu in.^2$$

$$S_{pf} = 0.176 \; \mu in.$$

$$3S_{pf} = 0.53 \; \mu in.$$

The 0.53 μin. is equivalent to 0.16 mm of pressure or 6.4% RH for a 10 inch block. The relative influence of the two parameters based on experience is approximately 1.5% RH variability and 0.13 mm pressure variability.

The effect of temperature measurement variability is maximized in the 10 inch steel block and minimized in the 10 inch glass-ceramic block. The difference in variance between these two blocks is 0.008 $\mu in.^2$ (0.048 - 0.040), attributable primarily to temperature variability and this is

equivalent to 0.002°C in a 10 inch steel block at the 3σ level.

This analysis shows the largest source of length dependent random error to be in the measurement of atmospheric pressure.

8.5. Summary

Application of single wavelength laser interferometry to reference standard gage blocks at NBS has proven valuable in several respects: (1) the extreme coherence of the light simplifies interferometry on blocks, especially those longer than 10 inches, (2) the bright, high contrast fringe patterns facilitate photographic recording and objective measurement, (3) the advent of ultra stable lasers reduces wavelength uncertainties, and (4) the special requirements in monitoring reference standard gage blocks make the process especially useful. The necessity for prior knowledge of gage block length to within 1/4 wavelength is the one drawback, although a minor one at NBS.

During this study of the long gage block process each random and systematic error source was minimized by improving equipment and techniques. A new process now exists because of these improvements and this new process will continue to be monitored. Performance during the last 8 months with the iodine stabilized laser indicates a measurement process in a state of statistical control (see fig. 10 and 11). The data show no statistically significant dependence on parameters which are potential systematic error sources indicating that systematic errors can be regarded as negligible relative to the random errors.

Evidence from the short control block measurements sets a probable limit on precision for this process at about 3σ=0.3 microinch. A possibility exists that using photo scanning techniques in fringe interpretation can improve precision, but the benefits will probably be small. Length dependent random errors can best be improved with better pressure measuring devices.

The one random error source not studied here, wringing variability, is now under analysis. In all probability it will be the largest single source of random err-

REFERENCES

[1] Pontius, P. E., The measurement assurance program - a case study, part I, short gage blocks (0.1 to 4 inches), Nat. Bur. Stand. (U.S.), Monogr. 149 (1975) in print.

[2] Pontius, P. E., The measurement assurance program - a case study, Part II, long gage blocks (5 to 20 inches), Nat. Bur. Stand. (U.S.), Monogr. (in process).

[3] Bruce, C. F., Australian J. Phys. 8:224 (1955).

[4] Thornton, B. S., Australian J. Phys. 8:241 (1955).

[5] Mielenz, K. D., et al, Appl. Opt. Vol. 7, No. 2:289 (1968).

[6] Schweitzer, W. G., et al, Appl. Opt. Vol. 12, No. 12:2927 (1973).

[7] Riddle, J. L., et al, Platinum resistance thermometry, Nat. Bur. Stand. (U.S.), Monogr. 126 (1973).

[8] Handegord, G. O., et al, Humidity and Moisture, Vol. I, Reinhold Publ. Corp., N.Y., 265 (1963).

[9] Hedlin, C. P., Humidity and Moisture, Vol. I, Reinhold Publ. Corp., N.Y., 273 (1963).

[10] Edlén, B., Metrologia, Vol. 2, No. 2, 71 (1966).

[11] Wexler, A. and Hasegawa, S., Relative humidity - temperature relationships of some saturated salt solutions, J. Res. Nat. Bur. Stand. (U.S.), Vol. 53, No. 1:19 (1954).

APPENDIX

Calibration Schedule

The apparatus used in the measurement of gage blocks during the period covered by this paper were calibrated and verified as follows:

1. Lasers

Laser No. 109: λ_0 was determined just before period A. Two previous determinations were made 19 and 18 months, respectively, before the start of this study. Variations in λ_0 of 1 part in 10^8 were observed among the three calibrations. The plasma tube in this laser failed during period G.

Laser No. 184: λ_0 was determined just before period H and again before period Q. A change of 13 parts in 10^8 occurred between calibrations.

Iodine stabilized laser: λ_0 was taken from published results [6]. The λ_0 of this laser will not change from the published value and its stated uncertainty as long as it is stabilized to the selected absorption line of iodine.

2. Hygrometer

The unit was calibrated by the manufacturer to within $\pm$ 1.5% RH just before period A and again in period H. No significant change was observed. At the end of this study the unit was tested against four saturated salt solutions [11] covering a range from 12% to 75% RH and the instrument readings agreed with the published values within 2% RH.

3. Aneroid barometer

Biweekly comparisons were made with a reference aneroid barometer maintained by the Pressure and Vacuum Section of NBS until period E. After period E comparisons were made with the reference barometer each time the control standard gage blocks were measured. During periods P and R several comparisons were also made with a fixed cistern mercury barometer. The accumulated data were used to calculate a mean correction to the aneroid. Only once (period D) did the mean correction change significantly.

4. Temperature measuring system

The SPRT, bridge, and thermocouples were calibrated just before period A. After rebuilding the system between B and C the bridge, thermocouples, and SPRT ice point were calibrated. Between G and H, and between P and Q, the SPRT ice point was redetermined, and the bridge was checked against a standard resistor. No significant changes were observed.

At the end of the study a further verification of the system was made. Two resistance bridges were used to measure temperature t of the insulated copper block with the SPRT. The first was the system Mueller bridge and the second was a high resolution a.c. bridge provided by the NBS Temperature Section. The procedure used was to measure R_t of the SPRT with both bridges (called A and B) in an A B B A sequence to compensate for the effect of temperature drift. Then the SPRT was placed in a triple point of water cell and R_o was measured with both bridges. Resistance ratio R_t/R_o and temperature t were computed from both sets of data and the SPRT constants. The average difference was 0.0004°C and the values had a range of 0.0003°C.

A test was also conducted to determine thermocouple effectiveness. Thermocouples were inserted into the holes of several blocks as described in Section 5 and, in addition, thermocouples were attached to the outside of the blocks with magnets. After overnight stabilization in the interferometer, the maximum difference observed between inside and outside block temperature was 0.0002°C and this value was not exceeded during three days of observation. Under adverse conditions, however, thermal contact between the thermocouples and the wall of the hole might need improving.